Current Biology, Volume *34*

Supplemental Information

A mismatch in the expression of cell surface molecules induces tissue-intrinsic defense against aberrant cells

Friedericke Fischer, Laurin Ernst, Anna Frey, Katrin Holstein, Deepti Prasad, Vanessa Weichselberger, Ramya Balaji, and Anne-Kathrin Classen

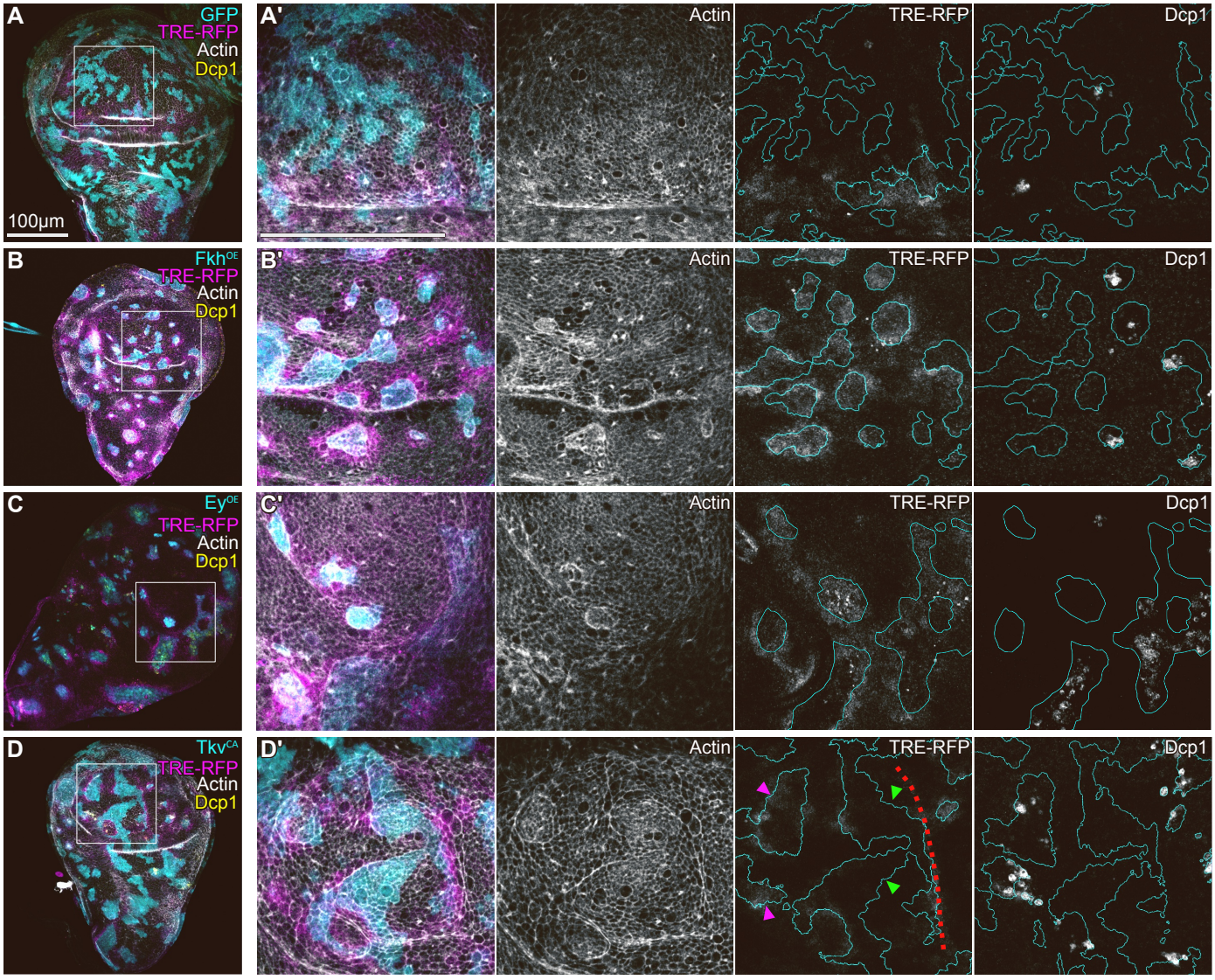

F

	OE	RNAi
Robo1	NA	
Robo2		
Robo3		
Slit		
Eph		
Ephrin		NA
Ten-m		
Ten-a		NA
Tl		
Toll2		
Toll3		
Toll4		
Toll5	NA	
Toll6		
Toll7		
Toll8		
Toll9	NA	
Ds		
Ft		
Dachs		
Caps	NA	
Trn		
NetB	NA	
Unc5	NA	
Fra		

	OE	RNAi
Rst		NA
Hbs		NA
Kirre		NA
PlexA		
PlexB	NA	
Sema2a	NA	
Ret		
Kek	NA	
Fwe$_{LoseA}$		NA
Fwe$_{LoseB}$		NA
GP150	NA	
Dscam4		
Dscam2	NA	
Pyd	NA	
Ics		NA
Sas	NA	
Fili	NA	
Bsg	NA	
Con	NA	
Beat-VII	NA	
Beat-IIIC	NA	
Tnc	NA	
Cirl	NA	

no TRE-RFP response
interface TRE-RFP response
other TRE-RFP responses
NA not assessed

Figure S1. Hallmarks of interface surveillance in response to clones with aberrant cell fate. Related to Figure 1.

A-D Mosaic wing disc with wild type clones expressing *UAS-GFP* (GFP) (A), or with clonal alterations in fate specifying pathways by ectopic expression of Fkh (Fkh^{OE}) (B), Ey (Ey^{OE}) (C), or expression of a constitutively active Tkv (Tkv^{CA}) (D) using the 'GAL4/UAS flp-out' system. TRE-RFP expression is reporting JNK pathway activity (grey or magenta in A-D). Antibody staining against the cleaved effector caspase (cDcp1) visualizes apoptosis (grey or yellow in A-D). Cortical F-actin was visualized by Phalloidin (grey). White frame marks regions shown in (A'-D').
Green and magenta arrows indicate clone interfaces in and outside Dpp signaling domain (E), respectively.

E Wing disc expressing the transcriptional reporter *dad*-LacZ, a target gene of the morphogen Dpp. Red dotted line represents the A/P compartment boundary. Previous work showed that Tkv^{CA} clones do not induce JNK boundary response in the Dpp-signaling domain (Prasad et al, 2023, Elife).

F Summary of the candidate screen for JNK interface signaling induced by either ectopic expression (^{OE}) of *UAS* constructs or downregulation of expression by *UAS-RNAi* (^{RNAi}) constructs for individual cell surface molecules (see **key resource table** for detailed constructs). The TRE-RFP reporter was used to access induction of JNK interface signaling at clone boundaries. Phenotypes of TRE-RFP responses were categorized in three groups: JNK interface signaling at clone boundaries (See **Figure 1** for representative images), other TRE-RFP responses (for example, intra-clonal activation) and no TRE-RFP responses (phenotypes not shown).

G-J Mosaic wing discs with aberrant expression of cell surface molecules. Clones express GFP (cyan) and were exposed to either ectopic expression (^{OE}) of *UAS* constructs or downregulation of expression by *UAS-RNAi* (^{RNAi}) constructs for individual cell surface molecules, as indicated in each panel. White frame marks regions shown in (G'-J').

Related images are shown at same scale with a scale bar of 100µm.

A

80 h | 102 h | 80 h | 102 h

Eph^{GFP} αPtc & αWg | Eph^{GFP} | Eph^{GFP} αPtc & αWg | Eph^{GFP} | Toll2^{GFP} αPtc & αWg | Toll2^{GFP} | Toll2^{GFP} αPtc & αWg | Toll2^{GFP}

100μm | 100μm | 100μm | 100μm

Ten-m^{GFP} αPtc & αWg | Ten-m^{GFP} | Ten-m^{GFP} αPtc & αWg | Ten-m^{GFP} | Toll8^{YFP} αPtc & αWg | Toll8^{YFP} | Toll8^{YFP} αPtc & αWg | Toll8^{YFP}

Ten-a^{GFP} αPtc & αWg | Ten-a^{GFP} | Ten-a^{GFP} αPtc & αWg | Ten-a^{GFP} | Rst^{GFP} αPtc & αWg | Rst^{GFP} | Rst^{GFP} αPtc & αWg | Rst^{GFP}

trn-LacZ Dapi | *trn*-LacZ | *trn*-lacZ Dapi | *trn*-LacZ | Hbs^{GFP} αPtc & αWg | Hbs^{GFP} | Hbs^{GFP} αPtc & αWg | Hbs^{GFP}

Ft^{GFP} αPtc & αWg | Ft^{GFP} | Ft^{GFP} αPtc & αWg | Ft^{GFP} | *hbs*-LacZ αPtc & αWg | *hbs*-LacZ | *hbs*-LacZ αPtc & αWg | *hbs*-LacZ

αDs Actin | αDs | αDs Actin | αDs | Sns^{GFP} αPtc & αWg | Sns^{GFP} | Sns^{GFP} αPtc & αWg | Sns^{GFP}

ds-LacZ αPtc & αWg | *ds*-LacZ | *ds*-LacZ αPtc & αWg | *ds*-LacZ | Sema1^{GFP} αPtc & αWg | Sema1^{GFP} | Sema1^{GFP} αPtc & αWg | Sema1^{GFP}

Slit^{GFP} Actin | Slit^{GFP} | Slit^{GFP} Actin | Slit^{GFP} | αSema2 Actin | αSema2 | αSema2 Actin | αSema2

Robo2^{GFP} αPtc & αWg | Robo2^{GFP} | Robo2^{GFP} αPtc & αWg | Robo2^{GFP} | NetA^{GFP} αPtc & αWg | NetA^{GFP} | NetA^{GFP} αPtc & αWg | NetA^{GFP}

αRobo1 Actin | αRobo1 | αNrt Actin | αNrt | αNrt Actin | αNrt

αRobo3 Ecad | αRobo3

100μm

B

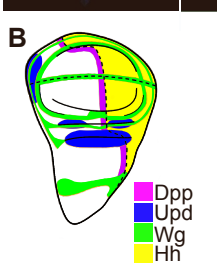

Figure S2. Expression patterns of cell surface molecules. Related to Figure 2.

A Wing discs expressing GFP-tagged fusion proteins or LacZ transcriptional reporters or stained with antibodies to detect protein expression patterns at 80 h and 102 h AEL. Ptc and Wg demarcate A/P and D/V compartment boundaries. F-actin visualizes wing disc area. All 80 h AEL discs are displayed at the same scale. All 102 h AEL discs are displayed at the same scale.

B Illustration of expression domains of fate-specifying signaling ligands, i.e., the morphogens Dpp (magenta), Wg (green), Hh (yellow) and Upd (blue). Please note that fate specifying signaling ligands also act non-autonomously by establishing morphogen gradients, and thereby specify fate patterns in the wing discs.

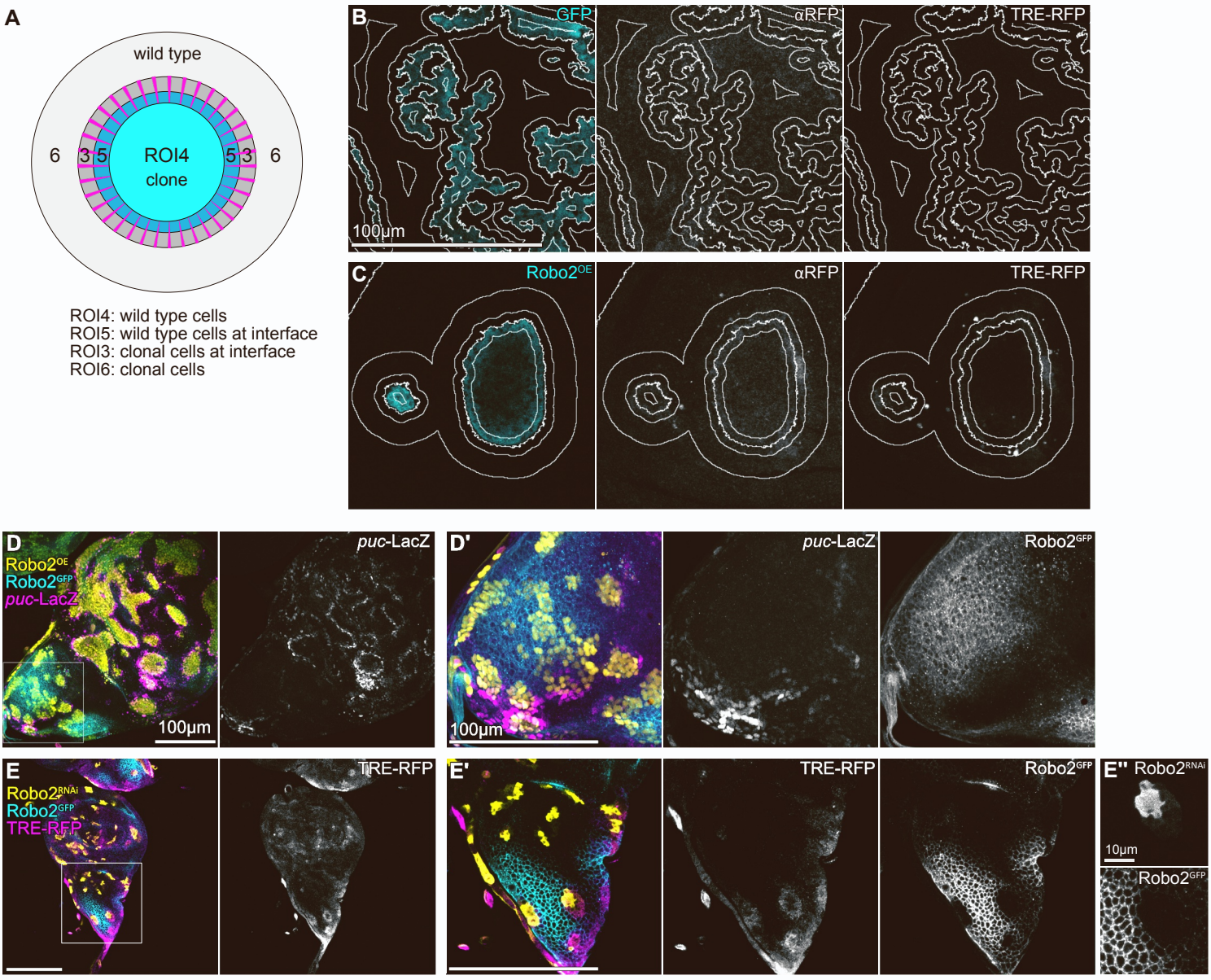
A
wild type
6
3
5
ROI4
clone
5
3
6
ROI4: wild type cells
ROI5: wild type cells at interface
ROI3: clonal cells at interface
ROI6: clonal cells
B
GFP
αRFP
TRE-RFP
100μm
C
Robo2OE
αRFP
TRE-RFP
D
Robo2OE
Robo2GFP
puc-LacZ
100μm
puc-LacZ
D'
puc-LacZ
Robo2GFP
100μm
E
Robo2RNAi
Robo2GFP
TRE-RFP
TRE-RFP
E'
TRE-RFP
Robo2GFP
E''
Robo2RNAi
10μm
Robo2GFP

Figure S3. Pattern-specific interface surveillance responses. Related to Figure 3.

A Illustration of segmented regions of interests (ROIs) as also described in (**Figure 3F**): clonal cells, that are not in touch with the interface (ROI4), a 4µm band of clonal cells (ROI5) and wild type cells (ROI3) at the interface and a 12µm band of wild type cells (ROI6) surrounding the previous ROIs (see Methods). Segmentation of the clonal interface provides the starting point for ROI annotation and subsequent measurements.

B,C Mosaic wing discs with *UAS-GFP* expressing (D) or *UAS-robo2* ($Robo2^{OE}$) (E) expressing clones. TRE-RFP expression is reporting JNK pathway activity. In addition to native TRE-RFP signal, anti-RFP antibody (αRFP) was used to enhance the TRE-RFP signal. White lines represent ROI segmentation.

D,E Wing discs expressing the *robo2-GFP* fusion protein ($Robo2^{GFP}$) under native regulatory control (grey or cyan). Mosaic clones (yellow) were induced that either express *UAS-robo2* ($Robo2^{OE}$) (D) or downregulate Robo2 using expression of *UAS-robo2-RNAi* ($Robo2^{RNAi}$) (E). Please note the reduced Robo2 expression level within clones in (E''). *puc*-LacZ (D) or TRE-RFP (E) expression (grey or magenta) is reporting JNK pathway activity (grey or magenta). Image sets are shown at the same scale. White frame marks region shown in (D', E').

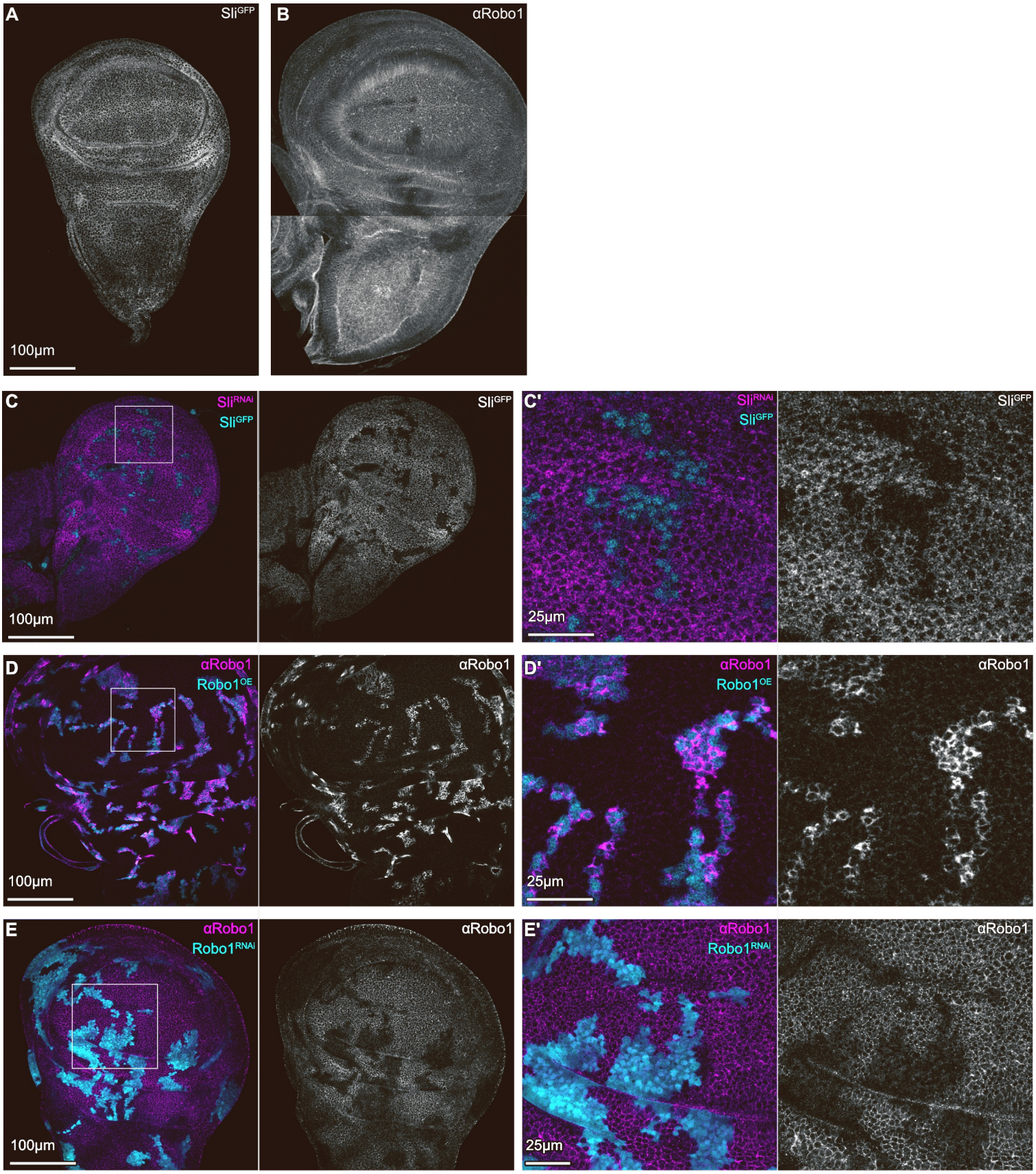
A
Sli^GFP
100µm
B
αRobo1
C
Sli^RNAi
Sli^GFP
100µm
Sli^GFP
C'
Sli^RNAi
Sli^GFP
25µm
Sli^GFP
D
αRobo1
Robo1^OE
100µm
αRobo1
D'
αRobo1
Robo1^OE
25µm
αRobo1
E
αRobo1
Robo1^RNAi
100µm
αRobo1
E'
αRobo1
Robo1^RNAi
25µm
αRobo1

Figure S4. Validation of Slit and Robo1 genetic constructs. Related to Figure 4.

A Wing disc expressing *Sli-GFP* (Sli^{GFP}) fusion protein construct under native regulatory control.

B Wing disc stained with an antibody to detect protein expression patterns of Robo1 (αRobo1).

C Mosaic wing disc expressing *Sli-GFP* (Sli^{GFP}) (magenta or grey) fusion protein construct under native regulatory control with clones (cyan) expressing *UAS-sli-RNAi* (Sli^{RNAi}). White frame marks region shown to the right in (C').

D, E Mosaic wing discs with clones (cyan) expressing *UAS-Robo1* ($Robo1^{OE}$) (D) or *UAS-Robo1-RNAi* ($Robo1^{RNAi}$) (E) stained with an antibody to detect protein expression of Robo1 (αRobo1) (magenta or grey). White frame marks region shown in (D' and E').

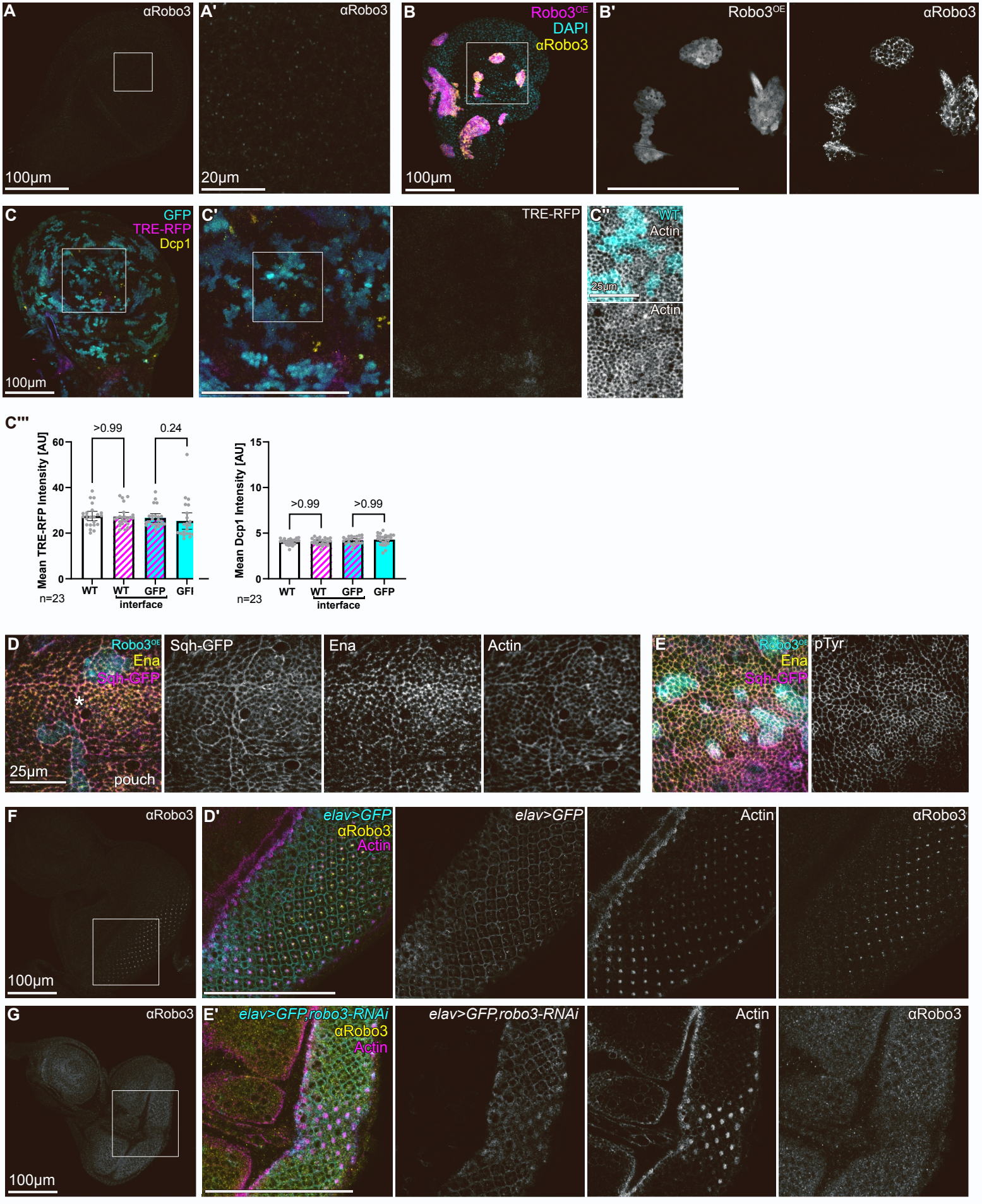
A
αRobo3
100μm
A'
αRobo3
20μm
B
Robo3OE
DAPI
αRobo3
100μm
B'
Robo3OE
αRobo3
C
GFP
TRE-RFP
Dcp1
100μm
C'
TRE-RFP
C''
WT
Actin
25μm
Actin
C'''
Mean TRE-RFP Intensity [AU]
>0.99
0.24
WT
WT
GFP
GFI
interface
n=23
Mean Dcp1 Intensity [AU]
>0.99
>0.99
WT
WT
GFP
GFP
interface
n=23
D
Robo3OE
Ena
Sqh-GFP
25μm
pouch
Sqh-GFP
Ena
Actin
E
Robo3OE
Ena
Sqh-GFP
pTyr
F
αRobo3
100μm
D'
elav>GFP
αRobo3
Actin
elav>GFP
Actin
αRobo3
G
αRobo3
100μm
E'
elav>GFP,robo3-RNAi
αRobo3
Actin
elav>GFP,robo3-RNAi
Actin
αRobo3

Figure S5. Validation of genetic tools for Robo3. Related to Figure 5.

A Wing imaginal disc stained by an anti-Robo3 antibody to visualize low level expression and punctate localization of Robo3. White frame marks region shown in (A').

B Mosaic wing disc with clones (magenta or grey) expressing *UAS-robo3* (Robo3^{OE}) and stained by an anti-Robo3 (αRobo3) (yellow or gray) antibody and DAPI (cyan or grey). White frame marks region shown in (B').

C A mosaic wing disc with wild type clones expressing *UAS-GFP* (GFP, cyan). TRE-RFP expression is reporting JNK pathway activity (grey or magenta). Antibody staining against the cleaved effector caspase (cDcp1) visualizes apoptosis (yellow). Phalloidin visualizes cortical F-actin (grey). White frame marks region shown in (C'). Please note that JNK activity is physiologically elevated at the A/P compartment boundary in wing discs at this developmental stage.

C''' Graph depicting mean fluorescence intensity of TRE-RFP reporter and mean cDcp1 intensity in the zones of measurement around clones, as depicted in (**Figure 3F**). Graphs display results for mosaic discs containing *UAS-GFP* (GFP) expressing clones. See **Figure 5** for comparison with other genotypes.
Sample number (n) for individual wing discs and p-values of a repeated measured one-way ANOVA with Tukey's multiple comparisons test are displayed in graphs. Error bars represent mean and 95% confidence interval.

D,E Mosaic wing disc with clones expressing *UAS-RFP* and *UAS-robo3* (Robo3^{OE}) (cyan) in the pouch of a wing disc. In (D): A GFP-tagged Non-muscle Myosin II regulatory light chain (Sqh-GFP) tracks the actin motor Myosin II. Antibody staining against Enabled (Ena) visualizes localization of the Drosophila Ena/Vasp actin polymerase. Phalloidin visualizes cortical F-actin. In (E): Antibody staining against phosphorylated Tyrosine (pTyr) is thought to visualize enhanced signaling activity at cellular junctions. The star marks the endogenous anterior-posterior compartment boundary. Image sets are shown at the same scale. Projections of the apical junctional network were generated using the LocalZ-projector.

F,G Eye imaginal discs with *elav*-GAL4 driven expression of *UAS-GFP* (F) or *UAS-GFP* and *UAS-robo3-RNAi* (G). Robo3 was visualized using an anti-Robo3 (αRobo3) antibody. Phalloidin visualizes cortical F-actin. Please note that Robo3 localizes to the center of assembling ommatidia clusters, which is reduced by expression of *robo3-RNAi*. White frame marks region shown in (F', G'). Image sets are shown at the same scale in (F,G) and (F',G') with a scale bar of 100µm.

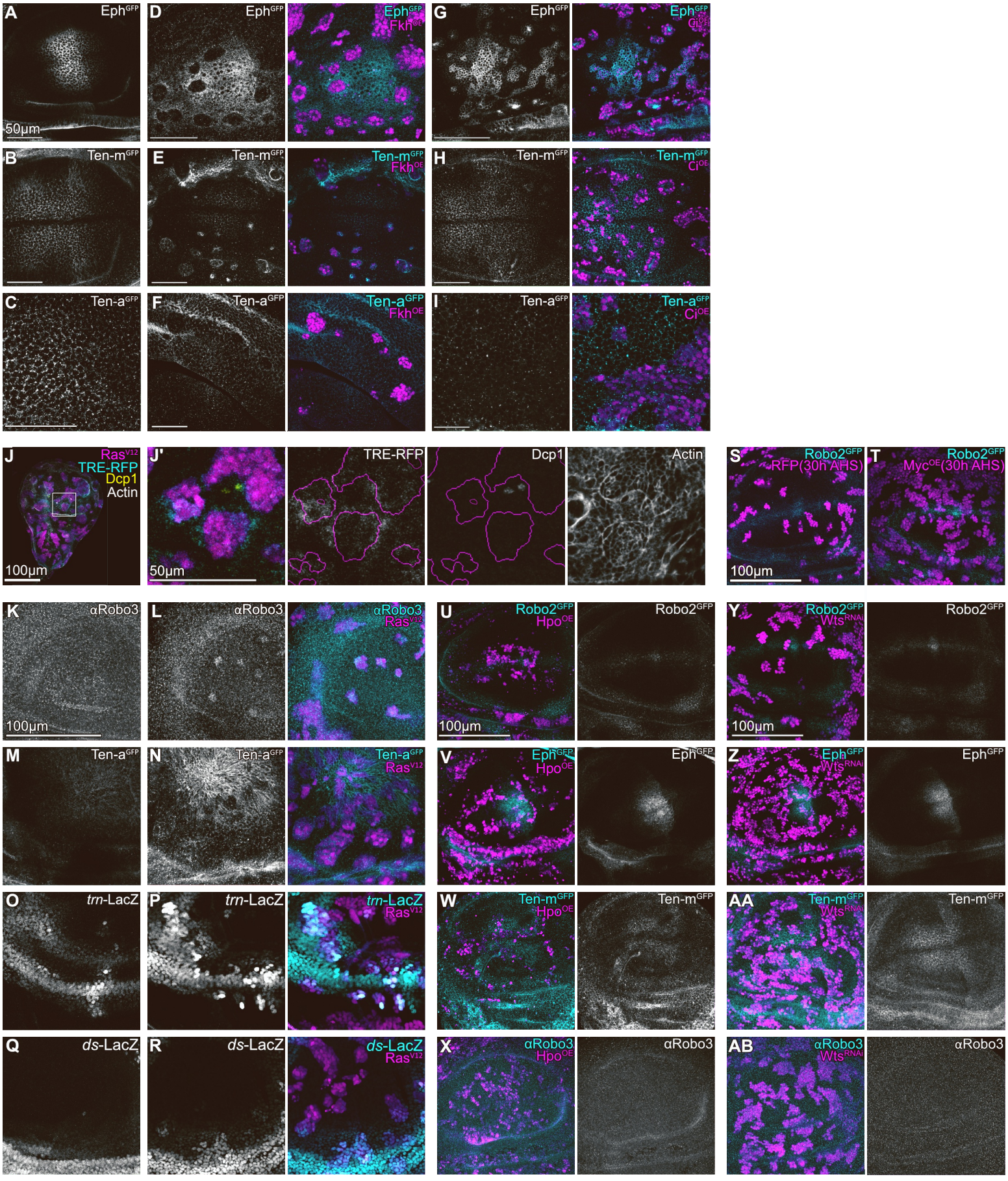
A
Eph^GFP
50μm
D
Eph^GFP
Eph^GFP Fkh^OE
G
Eph^GFP
Eph^GFP Ci^OE
B
Ten-m^GFP
E
Ten-m^GFP
Ten-m^GFP Fkh^OE
H
Ten-m^GFP
Ten-m^GFP Ci^OE
C
Ten-a^GFP
F
Ten-a^GFP
Ten-a^GFP Fkh^OE
I
Ten-a^GFP
Ten-a^GFP Ci^OE
J
Ras^V12
TRE-RFP
Dcp1
Actin
100μm
J'
50μm
TRE-RFP
Dcp1
Actin
S
Robo2^GFP
RFP(30h AHS)
100μm
T
Robo2^GFP
Myc^OE(30h AHS)
K
αRobo3
100μm
L
αRobo3
αRobo3 Ras^V12
U
Robo2^GFP Hpo^OE
Robo2^GFP
100μm
Y
Robo2^GFP Wts^RNAi
Robo2^GFP
100μm
M
Ten-a^GFP
N
Ten-a^GFP
Ten-a^GFP Ras^V12
V
Eph^GFP Hpo^OE
Eph^GFP
Z
Eph^GFP Wts^RNAi
Eph^GFP
O
trn-LacZ
P
trn-LacZ
trn-LacZ Ras^V12
W
Ten-m^GFP Hpo^OE
Ten-m^GFP
AA
Ten-m^GFP Wts^RNAi
Ten-m^GFP
Q
ds-LacZ
R
ds-LacZ
ds-LacZ Ras^V12
X
αRobo3 Hpo^OE
αRobo3
AB
αRobo3 Wts^RNAi
αRobo3

Figure S6. Expression of cell surface molecules in wing discs is regulated by fate-patterning pathways but not by cell competition. Related to Figure 6.

A-C Wing discs presenting the specific expression patterns of *eph-GFP* (Eph^{GFP}) (A), *ten-m-GFP* ($Ten\text{-}m^{GFP}$) (B) or *ten-a-GFP* ($Ten\text{-}a^{GFP}$) (C) serving as a reference pattern for the experimentally induced changes in (D-I).

D-I Wing discs expressing *eph-GFP* (Eph^{GFP}) (D), *ten-m-GFP* ($Ten\text{-}m^{GFP}$) (E), or *ten-a-GFP* ($Ten\text{-}a^{GFP}$) (F) (grey or cyan). Mosaic clones (magenta) deregulate fate-specifying pathway by expression of Fkh (Fkh^{OE}) (D-F) or by expression of Ci (Ci^{OE}) (G-I). Image sets are shown at the same scale with a scale bar of 50µm.

J Mosaic wing disc with clones deregulating EGF/ERK-signaling by expression of an oncogenic Ras, using the *UAS-RasV12* (Ras^{V12}) (magenta) construct. TRE-RFP expression is reporting JNK pathway activity (grey or cyan). Antibody staining against the cleaved effector caspase (cDcp1) visualizes apoptosis (grey or yellow). Phalloidin (grey) visualizes cortical F-actin. White frame marks region shown in (J'). Outline of clonal marker in magenta.

K,M,O,Q Wing discs presenting the specific expression patterns of Robo3 (αRobo3) (K), *ten-a-GFP* ($Ten\text{-}a^{GFP}$) (M), *trn-LacZ* (O) or *ds-LacZ* (Q), serving as a reference pattern for the experimentally induced changes in (L,N,P,R).

L,N,P,R Wing discs presenting the specific expression patterns of Robo3 (αRobo3) (L), *ten-a-GFP* ($Ten\text{-}a^{GFP}$) (N), *trn-LacZ* (P) *or ds-LacZ* (R) (grey or cyan) and carrying mosaic clones (magenta) expressing oncogenic *UAS-RasV12* (Ras^{V12}).

S,T Wing discs expressing *robo2-GFP* ($Robo2^{GFP}$), that carry mosaic clones expressing *UAS-RFP* (RFP) (S) or *UAS-Myc* (Myc^{OE}) (T). Both wing discs were dissected 30h after heat shock (AHS).

U-X Wing discs expressing *robo2-GFP* ($Robo2^{GFP}$) (U), *eph-GFP* (Eph^{GFP}) (V), *ten-m-GFP* ($Ten\text{-}m^{GFP}$) (W) or stained for Robo3 (X), and carrying mosaic clones expressing Hippo (Hpo^{OE}). Hippo expression reduces Yorkie function and thus, gives rise to loser cells.

Y-AB Wing discs expressing *robo2-GFP* ($Robo2^{GFP}$) (Y), *eph-GFP* (Eph^{GFP}) (Z), *ten-m-GFP* ($Ten\text{-}m^{GFP}$) (AA) or stained for Robo3 (AB), and carrying mosaic clones expressing *UAS-wts-RNAi* (wts^{RNAi}). Knocking down *warts* function activates Yorkie and thus gives rise to super competitor/winner cells.

Images (K-R) and (U-AB) are shown at the same scale.

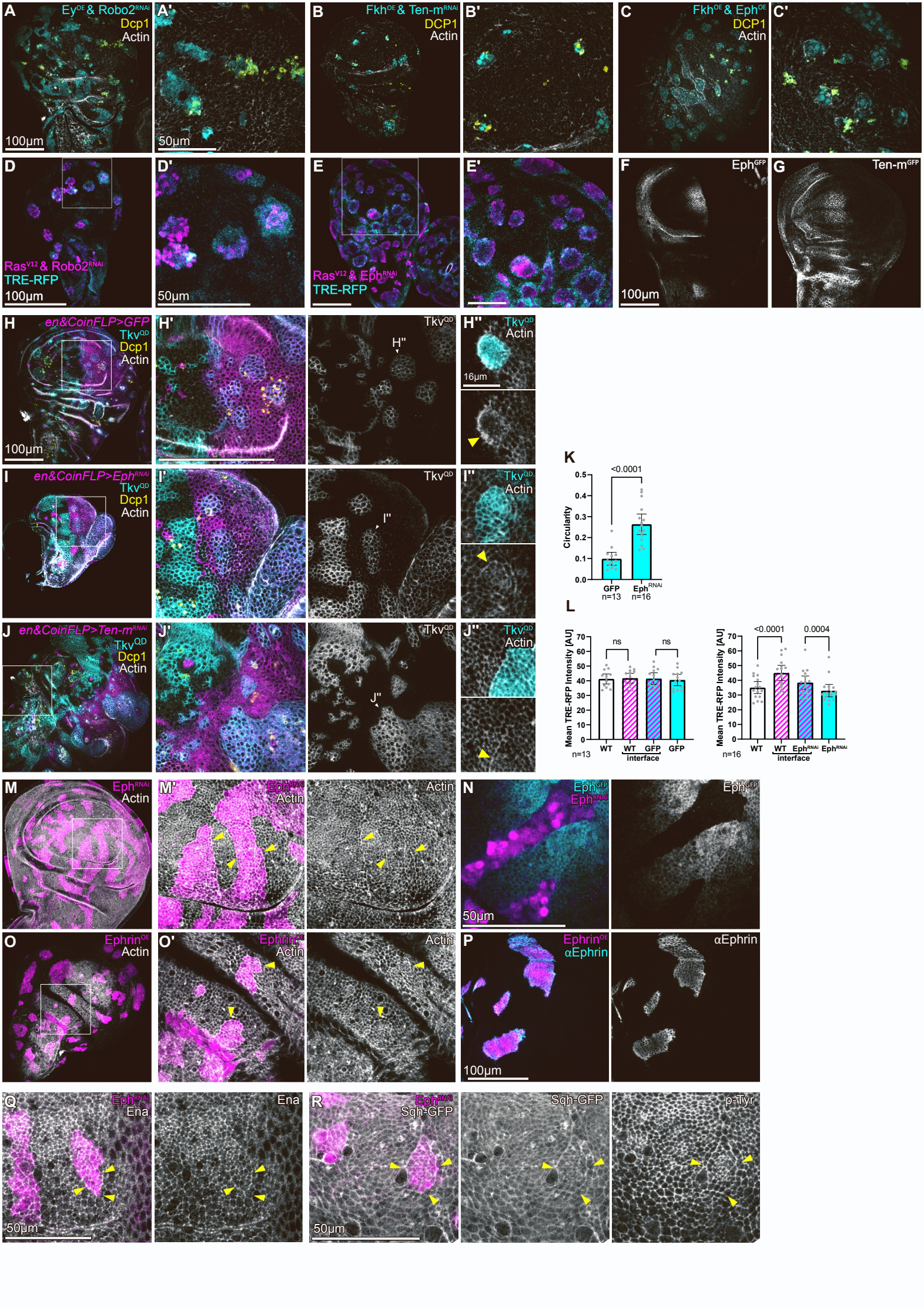
A
Ey^OE & Robo2^RNAi
Dcp1
Actin
100µm
A'
50µm
B
Fkh^OE & Ten-m^RNAi
DCP1
Actin
B'
C
Fkh^OE & Eph^OE
DCP1
Actin
C'
D
Ras^V12 & Robo2^RNAi
TRE-RFP
100µm
D'
50µm
E
Ras^V12 & Eph^RNAi
TRE-RFP
E'
F
Eph^GFP
100µm
G
Ten-m^GFP
H
en&CoinFLP>GFP
Tkv^QD
Dcp1
Actin
100µm
H'
Tkv^QD
H"
H''
Tkv^QD
Actin
16µm
I
en&CoinFLP>Eph^RNAi
Tkv^QD
Dcp1
Actin
I'
Tkv^QD
I"
I''
Tkv^QD
Actin
J
en&CoinFLP>Ten-m^RNAi
Tkv^QD
Dcp1
Actin
J'
Tkv^QD
J"
J''
Tkv^QD
Actin
K
<0.0001
Circularity
0.5
0.4
0.3
0.2
0.1
0.0
GFP
n=13
Eph^RNAi
n=16
L
Mean TRE-RFP Intensity [AU]
ns
ns
WT
WT
GFP
GFP
interface
n=13
<0.0001
0.0004
WT
WT
Eph^RNAi
Eph^RNAi
interface
n=16
M
Eph^RNAi
Actin
M'
Eph^RNAi
Actin
Actin
N
Eph^GFP
Eph^RNAi
50µm
Eph^GFP
O
Ephrin^OE
Actin
O'
Ephrin^OE
Actin
Actin
P
Ephrin^OE
αEphrin
100µm
αEphrin
Q
Eph^RNAi
Ena
50µm
Ena
R
Eph^RNAi
Sqh-GFP
50µm
Sqh-GFP
p-Tyr

Figure S7. Interface surveillance is redundantly mediated by multiple cell surface receptors. Related to Figure 6 and 7 and Data S4.

A-C Mosaic wing discs with clones deregulating a fate-specifying pathway and a cell surface receptor. Knock-down and overexpression constructs for cell surface receptors were selected to restore expression levels of the receptor within aberrant cells to wild type levels. Mosaic clones deregulating a fate-specifying pathway either express *UAS-ey* (Ey^{OE}) (A) or *UAS-fkh* (Fkh^{OE}) (B,C). To manipulate expression levels of cell surface receptors, we used *UAS-robo2-RNAi* ($Robo2^{RNAi}$) (A), *UAS-ten-m-RNAi* ($Ten\text{-}m^{RNAi}$) (B) or *UAS-Eph* (Eph^{OE}) (C). Antibody staining against the cleaved effector caspase (cDcp1) visualizes apoptosis (grey or yellow). Phalloidin visualizes cortical F-actin (grey). Basal sections are shown. Please note that clones still acquire a round smooth shape, and induce interface enrichment of actin and apoptosis.
A'-C' Magnified views of the pouch region of the wing disc. Images are shown at the same scale with a scale bar of 50µm.

D,E Mosaic wing discs with clones expressing oncogenic *UAS-RasV12* (Ras^{V12}) (magenta). The same clones either co-express *UAS-robo2-RNAi* ($Robo2^{RNAi}$) (D) or *UAS-eph-RNAi* (Eph^{RNAi}) (E). TRE-RFP expression is reporting JNK pathway activity (cyan). White frames marks regions shown in (D',E'). Please note that clones still acquire a round smooth shape and induce interface JNK signaling. Image sets are shown at the same scale in (D,E) and (D',E').

F, G Wing disc from larva with the genotype *CoinFLP-LexA::GAD.GAL4/hsflp^{122} ; en-GAL4/tub>CD2>GAL4, UAS-nLac ; UAS-eph-RNAi/eph-GFP* (F) for testing the genetic constructs used in (I), or a disc from larva with the genotype *CoinFLP-LexA::GAD.GAL4/+ ; en-GAL4/+ ; UAS-ten-m-RNAi/ten-m-GFP* (G) for testing the genetic constructs used in (J). No heat shock was applied hence only *en*-GAL4 is active in the posterior compartment. Please note downregulation of Eph (grey) and Ten-m (grey) in the posterior compartments indicating efficient RNAi-mediated knock-down.

H-J Mosaic wing discs with clones deregulating a fate-specifying pathway by expressing a constitutively active Tkv receptor (Tkv^{QD}) via the LexA/LexO-CoinFLP system (grey or cyan). *en*-GAL4 constitutively drives expression of UAS-constructs in the posterior compartment (magenta). The CoinFLP induces either LexA or GAL4 clones upon Flp-FRT recombination. Therefore GAL4/UAS clones expressing *UAS-GFP* (GFP) can also occasionally be observed in the anterior compartment. All GAL4-expressing cells (magenta) drive knock-down of cell surface molecules by expression of *UAS-eph-RNAi* (Eph^{RNAi}) (I) *or UAS-ten-m-RNAi* ($Ten\text{-}m^{RNAi}$) (J). Antibody staining against the cleaved effector caspase (cDcp1) visualizes apoptosis (grey or yellow). Phalloidin visualizes cortical F-actin (grey). White frames mark regions shown in (H'-J'). Images are shown at the same scale in (H-J) and (H'-J'). Representative wing discs of $n \geq 5$ wing discs from $n = 2$ experimental replicates are shown.

H''-J'' Magnified view of clones in the posterior compartment marked in (H'-J'). An apical section is shown. Please note the actin enrichment at clonal interfaces (yellow arrows). Images are shown at the same scale.

K Graph depicting circularity observed for individual *UAS-GFP* (GFP) and *UAS-eph-RNAi* (Eph^{RNAi}) expressing clones. Sample number (n) for individual wing discs and p-values of a two tailed, unpaired t-test are displayed in graphs. Error bars represent mean and 95% confidence interval.

L Graphs depicting mean fluorescence intensity of TRE-RFP reporter in zones of measurement around clones, as depicted in (**Figure 3F**). Graphs display results for mosaic discs with *UAS-GFP* labeled clonal cells (left) or containing *UAS-eph-RNAi* (Eph^{RNAi}) expressing clones (right). Sample number (n) for individual wing discs and p-values of a repeated measured one-way ANOVA with Tukey's multiple comparisons test are displayed in graphs. Error bars represent mean and 95% confidence interval.

M Mosaic wing disc carrying clones expressing *UAS-eph-RNAi* (Eph^{RNAi}) (magenta) to induce downregulation of Eph-receptor. Please note enrichment of F-actin at the clone interface (yellow arrows). White frame marks region shown in (M').

N A wing disc expressing *eph-GFP* (Eph^{GFP}) and carrying mosaic clones *UAS-eph-RNAi* (Eph^{RNAi}) to induce downregulation of the Eph-receptor. Please note the strong downregulation of Eph in clones, demonstrating efficiency of knock-down using *UAS-eph-RNAi* (Eph^{RNAi}).

O Mosaic wing disc carrying clones expressing UAS-ephrin ($Ephrin^{OE}$) to express high levels of Ephrin. An apical section is shown. Please note enrichment of F-actin at the clone interface (yellow arrows). White frame marks region shown in (O').

P Mosaic wing disc with clones expressing *UAS-ephrin* ($Ephrin^{OE}$) and stained with an antibody against Ephrin (αEphrin).

Q, R Mosaic wing discs carrying clones expressing *UAS-eph-RNAi* (Eph^{RNAi}) (magenta) to induce downregulation of Eph-receptor. Please note enrichment of Enabled (Ena) (Q) and the Myosin II regulatory light chain (Sqh-GFP), as well as phosphorylated Tyrosine (pTyr) (R) at the clone interface (yellow arrows).

Table S1

Figure	Genotype	Heat shock	Analysis after:
1A	*hsflp^{122}/+ ; TRE-RFP/+ ; act>y^{+}>GAL4, UAS-GFP/+*	10 min	48 h 25 °C
1B	*hsflp^{122}/UAS-fkh-3xHA ; TRE-RFP/+ ; act>y^{+}>GAL4, UAS-GFP/+*	10 min	30 h 25 °C
1C	*hsflp^{122}/+ ; TRE-RFP/+ ; act>y^{+}>GAL4, UAS-GFP/UAS-tkv^{CA}*	9 min	30 h 25 °C
1D	*hsflp^{122}/+ ; TRE-RFP/UAS-robo3-HA ; act>y^{+}>GAL4, UAS-GFP/+*	10 min	48 h 25°C
1E	*hsflp^{122}/+ ; TRE-RFP/UAS-robo2-HA ; act>y^{+}>GAL4, UAS-GFP/+*	8 min	48 h 25°C
1F	*hsflp^{122}/+ ; TRE-RFP/+ ; act>y^{+}>GAL4, UAS-GFP/UAS-robo2-RNAi*	10 min	48 h 25°C
1G	*hsflp^{122}/+ ; TRE-RFP/UAS-DEphrin ; act>y^{+}>GAL4, UAS-GFP/+*	10 min	30 h 25 °C
1H	*hsflp^{122}/+ ; TRE-RFP/+ ; act>y^{+}>GAL4, UAS-GFP/UAS-eph-RNAi*	7min	72h 25°C
1I	*hsflp^{122}/+ ; TRE-RFP/UAS-ten-a ; act>y^{+}>GAL4, UAS-GFP/+*	10min	48 h 25 °C
1J	*hsflp^{122}/+ ; TRE-RFP/UAS-ten-m ; act>y^{+}>GAL4, UAS-GFP/+*	10min	48 h 25 °C
1K	*hsflp^{122}/+ ; TRE-RFP/+ ; act>y^{+}>GAL4, UAS-GFP/UAS-ft*	10 min	48 h 25 °C
1L	*hsflp^{122}/+ ; TRE-RFP/+ ; act>y^{+}>GAL4, UAS-GFP/UAS-ft-RNAi*	10 min	48 h 25 °C
1M	*hsflp^{122}/+ ; TRE-RFP/UAS-ds^{A} ; act>y^{+}>GAL4, UAS-GFP/+*	10 min	48 h 25°C
1N	*hsflp^{122}/+ ; TRE-RFP/UAS-ds-RNAi ; act>y^{+}>GAL4, UAS-GFP/+*	10 min	48 h 25 °C
S1A	*hsflp^{122}/+ ; TRE-RFP/+ ; act>y^{+}>GAL4, UAS-GFP/+*	9 min	30 h 25 °C
S1B	*hsflp^{122}/UAS-fkh-3xHA ; TRE-RFP/+ ; act>y^{+}>GAL4, UAS-GFP/+*	10 min	30 h 25 °C
S1C	*hsflp^{122}/+ ; TRE-RFP/UAS-ey ; act>y^{+}>GAL4, UAS-GFP/+*	10 min	30 h 25 °C
S1D	*hsflp^{122}/+; TRE-RFP/+; act>y^{+}>GAL4, UAS-GFP/UAS-tkv^{CA}*	9 min	30 h 25 °C

S1E	*hsflp^{122}/+ ; TRE-RFP/dad^{4}-LacZ ; act>y^{+}>GAL4, UAS-GFP/+*	8.5 min	30 h 25°C
S1F	*Flylines from table S1 and S2 were crossed into flies with the genotype hsflp^{122} ; TRE-RFP ; act>y^{+}>GAL4, UAS-GFP*	10min	48 h 25 °C
S1G	*hsflp^{122}/+ ; TRE-RFP/UAS-toll-8 ; act>y^{+}>GAL4, UAS-GFP/+*	10 min	48 h 25 °C
S1H	*hsflp^{122}/+ ; TRE-RFP/+ ; act>y^{+}>GAL4, UAS-GFP/UAS-toll-2*	10 min	48 h 25 °C
S1I	*hsflp^{122}/+ ; TRE-RFP/UAS-netB-RNAi ; act>y^{+}>GAL4, UAS-GFP/+*	10 min	48 h 25 °C
S1J	*hsflp^{122}/+ ; TRE-RFP/UAS-trn-HA ; act>y^{+}>GAL4, UAS-GFP/+*	10 min	30 h 25 °C
3A	*hsflp^{122}/+ ; TRE-RFP/+ ; act>y^{+}>GAL4, UAS-GFP/+*	12 min	30 h 25°C
3B	*hsflp^{122}/+ ; TRE-RFP/UAS-robo2-HA ; act>y^{+}>GAL4, UAS-GFP/+*	12 min	30 h 25°C
3C	*hsflp^{122}/+ ; TRE-RFP/+ ; act>y^{+}>GAL4, UAS-GFP/UAS-robo2-RNAi*	14 min	30 h 25°C
S3B	*hsflp^{122}/+ ; TRE-RFP/+ ; act>y^{+}>GAL4, UAS-GFP/+*	8 min	48 h 25°C
S3C	*hsflp^{122}/+ ; TRE-RFP/UAS-robo2-HA ; act>y^{+}>GAL4, UAS-GFP/+*	8 min	48 h 25°C
S3D	*hsflp^{122}/+ ; TRE-RFP/robo2-GFP ; act>CD2>GAL4, UAS-RFP/puc$^{A251.1F3}$>LacZ*	11 min	30 h 25°C
S3E	*hsflp^{122}/CoinFLP-LexA::GAD.GAL4 ; TRE-RFP/robo2-GFP ; UAS-robo2-RNAi/UAS-LacZ*	14 min	30 h 25°C
4A	*hsflp^{122}/+ ; sqh-GFP/UAS-robo2-HA ; act>CD2>GAL4, UAS-RFP/+*	10 min	30 h 25°C
4B	*hsflp^{122}/+ ; sqh-GFP/UAS-robo2-HA ; act>CD2>GAL4, UAS-RFP/+*	10 min	30 h 25°C
4C	*hsflp^{122}/+ ; sqh-GFP/UAS-robo2-HA ; act>CD2>GAL4, UAS-RFP/+*	10 min	30 h 25°C
4D	*hsflp^{122}/+ ; sqh-GFP/UAS-robo2-HA ; act>CD2>GAL4, UAS-RFP/+*	10 min	30 h 25°C
4E	*hsflp^{122}/+ ; TRE-RFP/+ ; act>y^{+}>GAL4, UAS-GFP/UAS-HA-robo2.DeltaC*	10 min	30 h 25°C
4F	*hsflp^{122}/+ ; TRE-RFP/+ ; act>y^{+}>GAL4, UAS-GFP/UAS-HA-robo2.Delta-Ig1+2 (soure T- Evans)*	10 min	48 h 25°C
4G	*hsflp^{122}/+ ; TRE-RFP/+ ; act>y^{+}>GAL4, UAS-GFP/UAS-sli.D*	10 min	48 h 25°C

4H	*hsflp^{122}/+ ; TRE-RFP/UAS-sli-RNAi ; act>y^{+}>GAL4, UAS-GFP/+*	10 min	30 h 25°C
4I	*hsflp^{122}/+ ; TRE-RFP/+ ; act>y^{+}>GAL4, UAS-GFP/UAS-HA-robo1*	10 min	48 h 25°C
4J	*hsflp^{122}/+ ; TRE-RFP/UAS-robo1-RNAi ; act>y^{+}>GAL4, UAS-GFP/+*	10 min	48 h 25°C
S4C	*hsflp^{122}/+ ; sli-GFP/UAS-sli-RNAi; act>CD2>GAL4, UAS-RFP /+*	10 min	30 h 25°C
S4D	*hsflp^{122}/+ ; TRE-RFP/+ ; act>y^{+}>GAL4, UAS-GFP/UAS-HA-robo1*	10 min	48 h 25°C
S4E	*hsflp^{122}/+ ; UAS-robo1-RNAi/+ ; act>y^{+}>GAL4, UAS-GFP/+*	10 min	48 h 25°C
5A,F	*hsflp^{122}/+ ; TRE-RFP/UAS-robo3-HA ; act>y^{+}>GAL4, UAS-GFP/+*	12 min	30 h 25°C
5B,G	*hsflp^{122}/+ ; TRE-RFP/UAS-robo3-RNAi ; act>y^{+}>GAL4, UAS-GFP/+*	14 min	30 h 25°C
5C	*hsflp^{122}/+ ; TRE-RFP/UAS-robo2-HA ; act>y^{+}>GAL4, UAS-GFP/+*	12 min	30 h 25°C
5D	*hsflp^{122}/+ ; TRE-RFP/+ ; act>y^{+}>GAL4, UAS-GFP/UAS-robo2-RNAi*	14 min	30 h 25°C
5I,J	*hsflp^{122}/+ ; TRE-RFP/UAS-robo3-HA ; act>y^{+}>GAL4, UAS-GFP/UAS-robo2-RNAi*	13 min	48 h 25°C
S5B	*hsflp^{122}/+ ; UAS-robo3-HA/+ ; act>y^{+}>GAL4, UAS-GFP/+*	10 min	30 h 25°C
S5C	*hsflp^{122}/+ ; TRE-RFP/+ ; act>y^{+}>GAL4, UAS-GFP/+*	12 min	30 h 25°C
S5D	*hsflp^{122}/+ ; sqh-GFP/UAS-robo3-HA ; act>CD2>GAL4, UAS-RFP/+*	10 min	30 h 25°C
S5E	elav-GAL4, UAS-GFP/+ ; +/+ ; +/+	No HS	102 h AEL
S5F	elav-GAL4, UAS-GFP/+ ; UAS-robo3-RNAi/+ ; +/+	No HS	102 h AEL
6A,F	*hsflp^{122} ; UAS-Tkv-RNAi/ robo2-GFP ; act>CD2>GAL4, UAS-RFP / +*	18 min	48 h 25°C
6B	*hsflp^{122}/UAS-fkh-3xHA ; robo2-GFP/+ ; act>CD2>GAL4, UAS-RFP/+*	12 min	30 h 25°C
6C	*hsflp^{122}/+ ; robo2-GFP/UAS-ey ; act>CD2>GAL4, UAS-RFP/+*	10 min	30 h 25°C
6H	*hsflp^{122}/+ ; tub>CD2>GAL4, UAS-nLacZ/+ ; eph-GFP/UAS-tkv^{CA}*	10 min	30 h 25°C
6J	*hsflp^{122}/+ ; tub>CD2>GAL4, UAS-nLacZ/+ ; ten-m-GFP/UAS-tkv^{CA}*	10 min	30 h 25°C
6L	*hsflp^{122}/ten-a-GFP ; +/tub>CD2>GAL4, UAS-nLacZ ; UAS-tkv^{CA}/+*	12 min	30 h 25°C

6N	*hsflp^{122} ; UAS-Tkv-RNAi/+ ; act>CD2>GAL4, UAS-RFP / trn-LacZ*	11 min	40 h 25°C
6P	*hsflp^{122}/+ ; robo2-GFP/UAS-Ras^{V12} ; act>CD2>GAL4, UAS-RFP/+*	10 min	30 h 25°C
6R	*hsflp^{122}/+ ; tub>CD2>GAL4, UAS-nLacZ/+ ; eph-GFP/UAS-Ras^{V12}*	10 min	30 h 25°C
6T	*hsflp^{122}/+ ; tub>CD2>GAL4, UAS-nLacZ/+ ; ten-m-GFP/UAS-Ras^{V12}*	10 min	30 h 25°C
6U	*hsflp^{122}/+ ; robo2-GFP/+ ; act>CD2>GAL4, UAS-RFP/+*	9.5 min	30 h 25°C
6V	*hsflp^{122}/+ ; robo2-GFP/+ ; act>CD2>GAL4, UAS-RFP/UAS-myc*	9.5 min	30 h 25°C
6W	*hsflp^{122}/+ ; tub>CD2>GAL4, UAS-nLacZ/+ ; eph-GFP/+*	9.5 min	30 h 25°C
6X	*hsflp^{122}/+ ; tub>CD2>GAL4, UAS-nLacZ/+ ; eph-GFP/UAS-myc*	9.5 min	30 h 25°C
6Y	*hsflp^{122}/+ ; tub>CD2>GAL4, UAS-nLacZ/+ ; ten-m-GFP/+*	9.5 min	30 h 25°C
6Z	*hsflp^{122}/+ ; tub>CD2>GAL4, UAS-nLacZ/+ ; ten-m-GFP/UAS-myc*	9.5 min	30 h 25°C
S6D	*hsflp^{122}/UAS-fkh-3xHA ; +/+ ; act>CD2>GAL4, UAS-RFP/eph-GFP*	10 min	30 h 25°C
S6E	*hsflp^{122}/UAS-fkh-3xHA; tub>CD2>GAL4, UAS-nLacZ/+ ; ten-m-GFP/+*	10 min	30 h 25°C
S6F	*ten-a-GFP/UAS-fkh-3xHA; hsflp^{38}/+ ; act>CD2>GAL4, UAS-RFP/+*	1 h	40 h 25°C
S6G	*hsflp^{122}/+ ; tub>CD2>GAL4, UAS-nLacZ/+ ; eph-GFP/UAS-ci-HA*	10 min	30 h 25°C
S6H	*hsflp^{122}/+ ; tub>CD2>GAL4, UAS-nLacZ/+ ; ten-m-GFP/UAS-ci-HA*	10 min	30 h 25°C
S6I	*hsflp^{122}/ten-a-GFP ; tub>CD2>GAL4, UAS-nLacZ/+ ; UAS-ci-HA/+*	13 min	30 h 25°C
S6J	*hsflp^{122}/+ ; TRE-RFP/+ ; act>y^{+}>GAL4, UAS-GFP/UAS-Ras^{V12}*	9 min	30 h 25°C
S6L	*hsflp^{122}/+ ; +/+ ; act>CD2>GAL4, UAS-RFP/ UAS-Ras^{V12}*	12 min	30 h 25°C
S6N	*hsflp^{122}/ten-a-GFP ; +/+ ; act>CD2>GAL4, UAS-RFP/UAS-Ras^{V12}*	12 min	30 h 25°C
S6P	*hsflp^{122}/+ ; UAS-Ras^{V12}/+ ; act>CD2>GAL4, UAS-RFP/trn-LacZ*	12 min	30 h 25°C
S6R	*hsflp^{122}/+ ; ds-LacZ/+ ; act>y^{+}>GAL4, UAS-GFP/UAS-Ras^{V12}*	10 min	30 h 25°C
S6S	*hsflp^{122}/+ ; robo2-GFP/+ ; act>CD2>GAL4, UAS-RFP/+*	9.5 min	30 h 25°C
S6T	*hsflp^{122}/+ ; robo2-GFP/+ ; act>CD2>GAL4, UAS-RFP/UAS-myc*	9.5 min	30 h 25°C

S6U	*hsflp^{122}/+ ; robo2-GFP/+; act>CD2>GAL4, UAS-RFP/UAS-hpo*	12 min	30 h 25°C
S6V	*hsflp^{122}/+ ; tub>CD2>GAL4, UAS-nLacZ/+ ; eph-GFP/UAS-hpo*	12 min	30 h 25°C
S6W	*hsflp^{122}/+ ; tub>CD2>GAL4, UAS-nLacZ/+ ; ten-m-GFP/UAS-hpo*	12 min	30 h 25°C
S6X	*hsflp^{122}/+ ; tub>CD2>GAL4, UAS-nLacZ/+ ; +/UAS-hpo*	12 min	30 h 25°C
S6Y	*hsflp^{122}/+ ; robo2-GFP/+ ; act>CD2>GAL4, UAS-RFP/UAS-wtsRNAi*	9.5 min	30 h 25°C
S6Z	*hsflp^{122}/+ ; tub>CD2>GAL4, UAS-nLacZ/+ ; eph-GFP/UAS-wtsRNAi*	9.5 min	30 h 25°C
S6AA	*hsflp^{122}/+ ; tub>CD2>GAL4, UAS-nLacZ/+ ; ten-m-GFP/UAS-wtsRNAi*	9.5 min	30 h 25°C
S6AB	*hsflp^{122}/+ ; +/+ ; act>CD2>GAL4, UAS-RFP/UAS-wtsRNAi*	9.5 min	30 h 25°C
S7A	*hsflp^{122}/+ ; UAS-ey/+ ; act>y^{+}>GAL4, UAS-GFP /UAS-robo2-RNAi*	10 min	30 h 25°C
S7B	*hsflp^{122}/UAS-fkh-3xHA ; tub>CD2>GAL4, UAS-nLacZ/+ ; UAS-ten-m-RNAi/+*	10 min	30 h 25°C
S7C	*hsflp^{122}/UAS-fkh-3xHA ; UAS-eph/+ ; act>CD2>GAL4, UAS-RFP/+*	12 min	30 h 25°C
S7D	*hsflp^{122}/+ ; tub>CD2>GAL4, UAS-nLacZ/TRE-RFP ; UAS-robo2-RNAi/UAS-Ras^{V12}*	10 min	30 h 25°C
S7E	*hsflp^{122}/+ ; TRE-RFP/UAS-Ras^{V12} ; act>y^{+}>GAL4, UAS-GFP/UAS-eph-RNAi*	10 min	30 h 25°C
S7F	*CoinFLP-LexA::GAD.GAL4/hsflp^{122} ; en-GAL4/tub>CD2>GAL4, UAS-nLacZ ; UAS-eph-RNAi/eph-GFP*	No HS	108h AEL
S7G	*CoinFLP-LexA::GAD.GAL4/+ ; en-GAL4/+ ; UAS-ten-m-RNAi/ten-m-GFP*	No HS	108h AEL
S7H	*hsflp^{122}/CoinFLP-LexA::GAD.GAL4 ; en-GAL4/UAS-mCD8::GFP, LexO-mCherry::CAAX ; LexO-tkv^{QD}/+*	5 min	38 h 25°C
S7I	*hsflp^{122}/CoinFLP-LexA::GAD.GAL4 ; en-GAL4/UAS-mCD8::GFP, LexO-mCherry::CAAX ; LexO-tkv^{QD}/UAS-eph-RNAi*	5 min	38 h 25°C
S7J	*hsflp^{122}/CoinFLP-LexA::GAD.GAL4 ; en-GAL4/UAS-mCD8::GFP, LexO-mCherry::CAAX ; LexO-tkv^{QD}/UAS-ten-m-RNAi*	5 min	38 h 25°C
S7M	*hsflp^{122}/+ ; +/+ ; act>y^{+}>GAL4, UAS-GFP/UAS-eph-RNAi*	11 min	48h 25°C

S7N	*hsflp^{122}/+ ; tub>CD2>GAL4, UAS-nLacZ/+ ; eph-GFP/UAS-eph-RNAi*	15 min	72 h 25°C
S7O	*hsflp^{122}/+ ; TRE-RFP/UAS-DEphrin ; act>y^{+}>GAL4, UAS-GFP/+*	10 min	30 h 25 °C
S7P	*hsflp^{122}/+ ; UAS-DEphrin /+ ; act>y^{+}>GAL4, UAS-GFP/+*	10 min	30 h 25°C
S7Q	*hsflp^{122}/+ ; sqh-GFP/+ act>CD2>GAL4, UAS-RFP/ UAS-eph-RNAi*	10 min	30 h 25°C
S7P	*hsflp^{122}/+ ; sqh-GFP/+ act>CD2>GAL4, UAS-RFP/ UAS-eph-RNAi*	10 min	30 h 25°C

Table S1. Detailed genotypes per figure panel. Related to STAR methods.

Table S2

S1A’	*Overlay*: apical z-sections of actin and clonal marker. Basal z-sections of TRE-RFP. *Black and white images*: apical z-section of Actin. Basal z-sections of TRE-RFP and Dcp1.
S1B’	*Overlay:* local Z projection of apical actin, apical clonal marker, and apical to lateral TRE-RFP. *Black and white images:* local z projection of apical actin, basal max projection of TRE-RFP and Dcp1
S1C’	*Overlay:* apical z-sections of actin, clonal marker and TRE-RFP. *Black and white images:* apical z-section of actin and lateral z-section of TRE-RFP and Dcp1.
S1D’	*Overlay:* max projection of apical z-sections of actin, clonal marker and TRE-RFP. *Black and white images:* apical z-section of actin, lateral z-section of TRE-RFP and basal z-section of Dcp1.
S5C and S5C’	Basal z-section.
S5C’’	Max projection of 3 apical z-sections.
5A and 5A’	Lateral z-section of clonal marker and TRE-RFP. Basal z-section of Dcp1.
5A’’	Max projection of 3 apical z-sections.
5B and 5B’	Lateral z-section of clonal marker and TRE-RFP. Basal z-section of Dcp1.
5B’’	Max projection of 3 apical z-sections.
3A	Lateral z-section for clonal marker and TRE-RFP (different z-section for pouch and notum). Max projection of z-sections for Dcp1.
3A’ and 3A’’	Max projection of apical z-sections for Actin, a lateral z-section for TRE-RFP and clonal marker and max projection of z-sections for Dcp1.
3C	Lateral z-section.
3C’	Apical z-section for Actin and clonal marker. Lateral z-section for TRE-RFP and Dcp1.
3C’’	Max projection of lateral to basal z-sections.
3B	Basal z-section for TRE-RFP and clonal marker (different z-section for pouch and notum). Max projection of all z-sections for Dcp1.
3B’	max projection of 2 apical z-sections for Actin, TRE-RFP and clonal marker. Basal z-section for Dcp1.
3B’’	max projection of 2 apical z-sections for Actin. Lateral z-section for clonal marker and TRE-RFP. Max projection of all z-sections for Dcp1.
S7H-J	lateral z-section for LexA and Gal4 clonal marker and Actin. Max projection of basal z-sections for Dcp1.
S6J	Max projection of apical to lateral z-section in the hinge
6U-Z and S6S-AB	Local z projection of lateral z-section

Table S2. Selected z-positions for figure panels with overlay of channels from different z-positions. Related to STAR methods.

In most figure panels, individual channels represent the same z-position from a confocal image stack. However, some panels may assemble channels from different z-position in the wing disc (details below). Such a portrayal was chosen to better visualize the spatially distinct phenotypes at different z-positions within the tissue, specifically of (1) junctional actin (apical), (2) cytoplasmic/nuclear RFP (lateral) and (3)

cDcp1 (basal) in one image panel. This was meant to reduce the data load in the manuscript that would be otherwise required to visualize all channels at all z-positions. All full original image stacks are of course available upon request.